

## Original Research

## Composition analysis and mechanism of Guizhi Fuling capsule in anti-cisplatin-resistant ovarian cancer

Lei Dou<sup>b</sup>, Yan Yan<sup>b</sup>, Enting Lu<sup>b</sup>, Fangmei Li<sup>b</sup>, Dongli Tian<sup>b</sup>, Lei Deng<sup>b</sup>, Xue Zhang<sup>b</sup>,  
Rongjin Zhang<sup>b</sup>, Yin Li<sup>c</sup>, Yi Zhang<sup>b,\*</sup>, Ye Sun<sup>a,\*</sup>

<sup>a</sup> Department of Pathogenic Biology, College of Basic Medical Sciences, Shenyang Medical College, Shenyang 110034, China

<sup>b</sup> Department of Gynecology, the First Hospital of China Medical University, Shenyang 110001, China

<sup>c</sup> Department of Integration of Chinese and Western Medicine, School of Basic Medical Sciences, Peking University, Beijing 100191, China

## ARTICLE INFO

## Keywords:

Ovarian cancer  
Cisplatin resistance  
EMT  
Metastasis  
PA2G4

## ABSTRACT

**Objective:** Cisplatin is the main chemotherapy drug for advanced ovarian cancer, but drug resistance often occurs. The aim of this study is to explore the molecular mechanism by which Guizhi Fuling capsule inhibits cisplatin resistance in ovarian cancer. **Methods:** First, differences in cisplatin resistance, PA2G4 gene expression, migration, and invasion in A2780 cells and A2780/DDP cells were analyzed by qRT-PCR, scratch assay, transwell, immunofluorescence, and western blotting. Then, LC-MS/MS analysis of GFC chemical composition. qRT-PCR, scratch tests, transwell, pseudopodium formation, immunofluorescence, and western blotting were used to explore the mechanism by which GFC inhibited A2780/DDP cell migration and invasion. Finally, the anti-tumor efficacy of GFC was verified by in vivo experiments. **Results:** A2780/DDP cells had a greater ability to migrate and invade compared to their parents. Cell viability experiments showed that the migration and invasion ability of A2780/DDP cells were significantly inhibited with the increase of GFC concentration. qRT-PCR results showed that compared with the blank control group, cisplatin group and GFC group, the transcription level of PA2G4 gene in the combination treatment group was significantly reduced. We also found that GFC combined with cisplatin inhibited the PI3K/AKT/GSK-3 $\beta$  signaling pathway by targeting PA2G4 gene expression, inhibited the epithelial-mesenchymal transition signaling pathway, decreased cell adhesion and inhibited the formation of cell pseudopodias. **Conclusion:** GFC combined with cisplatin can target PA2G4 gene to regulate PI3K/AKT/GSK-3 $\beta$  Signaling pathway, inhibiting the invasion and migration of cisplatin resistant A2780/DDP cells in ovarian cancer.

## Introduction

According to statistics, the mortality rate of ovarian cancer among women in the United States ranks fifth among all malignant tumors. Worldwide, 140,000 women die from ovarian cancer every year [1]. Due to the difficulty of recognizing early symptoms of ovarian cancer and the lack of diagnostic techniques, more than 70% of patients with ovarian cancer are at an advanced stage at the time of diagnosis [2,3]. At present, platinum-based combined chemotherapy is the main treatment method for patients with advanced ovarian cancer [4,5]; however, the resistance of ovarian cancer to cisplatin increases significantly after several chemotherapy cycles, which limits its clinical therapeutic effect [6–8]. Therefore, relying solely on existing technologies to improve the survival rate of patients offers limited results, and more effective

treatment methods need to be explored.

Epithelial–mesenchymal transition (EMT) refers to the transition of epithelial to mesenchymal cells, which endows cells with the ability to migrate and invade, and not only plays a key role in development, but also participates in the process of carcinogenesis [9–12]. Typical EMTs are characterized by dissolution of intercellular junctions, cytoskeletal rearrangement from keratin to Vimentin expression, disappearance of the typical polygonal or spindle-like appearance, and increased activity of mesenchymal cell markers N-Cadherin and matrix metalloproteinases. In addition, EMT is regulated by extracellular matrix components, exosomes, and soluble factors [13]. An increasing number of studies have shown that EMT and tumor cell drug resistance have a common signaling regulatory pathway, and the activation and dysregulation of EMT-related signaling pathways synergistically regulate the

\* Corresponding authors.

E-mail addresses: [syzi@163.com](mailto:syzi@163.com) (Y. Zhang), [sunye@symc.edu.cn](mailto:sunye@symc.edu.cn) (Y. Sun).

process of tumor cell interstitialization and tumor cell drug resistance [14–16]. EMT of cancer cells is thought to enhance their aggressiveness, generate circulating tumor cells and cancer stem cells, and promote resistance to anticancer drugs [17–19].

In recent years, with the development of bioinformatics, public databases such as Web of Science, PubMed and Embase have been continuously improved and updated. More and more researchers are using databases to explore new ways of cancer prevention and treatment. The Royal Marsden Hospital (RMH) score is based on blood tests and clinical characteristics of patients, and there is a negative correlation between RMH score and survival of cancer patients, and RMH score is expected to become a prognostic tool [20]. Immune checkpoint inhibitors (ICIs) are associated with a variety of immune-related adverse events (irAEs). This meta-analysis found that ICIs can evaluate the characteristics, performance, and treatment of tumors in patients with melanoma, endometrial cancer, and liver cancer [21–24].

Cinnamomum cassia and Poria cocos, the active pharmacological components of the traditional Chinese remedy Guizhi Fuling decoction (GFD), are the source of Guizhi Fuling capsule (GFC). GFC has the effects of inhibiting platelet aggregation and reducing blood viscosity, and it is widely used for the treatment of clinical uterine fibroids, chronic pelvic inflammatory disease and its mass, and irregular exfoliation of the endometrium [25,26]. Recent studies have found that GFC combined with chemotherapy drugs can increase the effect of antitumor treatment [27,28]. However, the exact antitumor mechanism of GFC remains unclear. In this study, we first evaluated the differences in migration and invasion ability and cisplatin resistance of human ovarian cancer cisplatin-sensitive cell line A2780 and cisplatin-resistant cell line A2780/DDP, and then explored the differences in the degree of cisplatin resistance. Increase the sensitivity of tumor cells to cisplatin by inhibiting EMT of A2780/DDP cells.

## Materials and methods

### Clinical data analysis

By searching the University of Alabama at Birmingham CANcer data (ULACAN, <http://ualcan.path.uab.edu/>) and entering the PA2G4 gene in the TCGA column, the clinical data including the expression of PA2G4 in normal tissues and various tumors, The expression of PA2G4 in various cancers, the expression of PA2G4 in ovarian tumors of different grades, the expression of PA2G4 in different advanced ovarian cancers, and the curve of PA2G4 gene and patient survival time. The expression of PA2G4 in different grades of ovarian tumors, the expression of PA2G4 in different advanced ovarian cancers and the curve of PA2G4 gene and patient survival time.

### Reagents and antibodies

Guizhi Fuling capsule (GFC) is a compound Chinese medicine (Jiangsu Kangyuan Pharmaceutical Co., Ltd., China) that includes Guizhi, Mudanpi, Taoren, Baishao, and Fuling. The ratio of the five drugs is 1:1:1:1:1, and the concentration of GFC crude drug was 0.31 g/capsule. Cisplatin was purchased from Sigma Aldrich Company (St. Louis, MO, USA). Primary antibodies included rabbit monoclonal anti-P13K (1:1000, Cat No. #4257), rabbit monoclonal anti-AKT (1:1000, Cat No. #4691), rabbit monoclonal anti-GSK-3 $\beta$  (1:1000, Cat No. #12,456), rabbit monoclonal anti-p-P13K (P85) (Tyr199, 1:1000, Cat No. #4228), rabbit monoclonal anti-p-AKT (Ser473, 1:1000, Cat No. #4058), and rabbit monoclonal anti-p-GSK-3 $\beta$  (1:1000, Cat No. #9323), rabbit monoclonal anti-LIMK1(1:1000, Cat No. #3842T), rabbit monoclonal anti-Cofilin(1:1000, Cat No. #5175T), rabbit monoclonal anti- $\alpha$ -Smooth Muscle Actin(1:1000, Cat No. #68463T) and were obtained from Cell Signaling Technology Inc. (Danvers, MA, USA). Rabbit polyclonal anti-E-cadherin (1:1000, Cat No. YT1454), rabbit polyclonal anti-N-cadherin (1:1000, Cat No. YT2988), rabbit polyclonal anti-MMP-2

(1:1000, Cat No. YT2798), rabbit polyclonal anti-Vimentin (1:1000, Cat No. YT4897), rabbit polyclonal anti-Snail (1:1000, Cat No. YT4351), and rabbit polyclonal anti-Slug (1:1000, Cat No. YT7985) were obtained from ImmunoWay Biotechnology Company (Plano, TX, USA).

### Cell lines and cell culture

The European Collection of Authenticated Cell Cultures (ECACC) provided the human ovarian cancer cell line (A2780), while the Beijing Dingguo Changsheng Biotechnology Corporation provided the human ovarian cancer cisplatin-resistant cell line (A2780/DDP) (Beijing, China). The cells were grown in DMEM/High Glucose (Hyclone, USA) with 10% fetal bovine serum, 100 U/mL penicillin, and 100 mg/mL streptomycin (Genview, Australia), and they were incubated at 37 °C in a 5% CO<sub>2</sub> environment. To maintain drug resistance, A2780/DDP cells were pulsed in media containing 2  $\mu$ g/mL cisplatin for at least 72 hours. Absence of cisplatin for two weeks before to the experiment can sustain cisplatin resistance in A2780/DDP cells for one month.

### Cell viability assay

A2780 cells and A2780/DDP cells totaling  $5 \times 10^3$ /well each were seeded onto 96-well plates, where they were then grown for 16 hours. After the density reaches 70%, the cell culture fluids should be discarded. The cells were treated for 24 h with cisplatin at various concentrations (4, 8, 16, 32, 64, and 128  $\mu$ g/mL) and GFC at different concentrations (9.375, 18.75, 37.5, 75, 150, and 300 mg/mL). Each plate received 10  $\mu$ L of the Cell Counting Kit-8 solution (Apexbio, USA) and was then incubated for 4 hours. At least three times were used to detect the 460 nm absorbance of each experiment. The cells cultured without drug were used as the control group, and the Cell Counting Kit-8 solution was used as the blank group. Cell viability was calculated as follows:  $(OD_{\text{experiment}} - OD_{\text{control}}) / (OD_{\text{control}} - OD_{\text{blank}}) \times 100\%$ . The IC<sub>5</sub> and IC<sub>50</sub> of cisplatin and Guizhi Fuling capsule were calculated by the curve-fitting method.

### EdU cell proliferation assay

A total of  $2 \times 10^5$  A2780/DDP cells were seeded into 6-well plates. The cells were divided into four groups, including the blank control group, the cisplatin single-action group (final concentration 3.743  $\mu$ g/mL, equivalent to IC<sub>5</sub>), the GFC single-action group (final concentration 0.063 mg/mL, equivalent to IC<sub>5</sub>), and the drug combination group (final concentration cisplatin 3.743  $\mu$ g/mL + GFC 0.063 mg/mL, equivalent to cisplatin IC<sub>5</sub> + GFC IC<sub>5</sub>). Different treatment conditions were applied to A2780/DDP cells for 24 h, after which 2 mL of 1  $\times$  EdU solution (final concentration, 10  $\mu$ M) was added and incubated for 2 h at room temperature. The cells were washed with phosphate-buffered saline (PBS) and fixed with 4% paraformaldehyde for 30 min. The cells were stained with EdU kit (Beyotime Biotechnology, Shanghai, China) and DAPI staining solution. Images were collected by fluorescence microscopy (Zeiss, Germany), and the number of cells stained by EdU and DAPI was counted by ImageJ software.

### Cell scratch assay

Briefly,  $2 \times 10^5$  cells/well A2780 cells and A2780/DDP were seeded in 6-well plates. After 16 h of adherence, they were scratched with a 1000- $\mu$ L pipette tip. Cells were incubated in different groups (blank control group: final concentration cisplatin 0  $\mu$ g/mL + GFC 0 mg/mL, cisplatin single-action group: final concentration 3.743  $\mu$ g/mL, GFC single-action group: final concentration 0.063 mg/mL, and drug combination group: final concentration cisplatin 3.743  $\mu$ g/mL + GFC 0.063 mg/mL), cultured them for 24 h, and fixed with 4% paraformaldehyde solution (Beyotime Biotechnology, China) for 60 min at room temperature. The experiment was repeated three times, and the cell scratch

area was calculated using ImageJ software.

#### Transwell cell migration assay

A2780/DDP cells were incubated in different groups (blank control group: final concentration cisplatin 0  $\mu\text{g}/\text{mL}$  + GFC 0  $\text{mg}/\text{mL}$ , cisplatin single-action group: final concentration 3.743  $\mu\text{g}/\text{mL}$ , GFC single-action group: final concentration 0.063  $\text{mg}/\text{mL}$ , and drug combination group: final concentration cisplatin 3.743  $\mu\text{g}/\text{mL}$  + GFC 0.063  $\text{mg}/\text{mL}$ ). Then, the cells were digested by trypsin, and collected by centrifugation at 1000 rpm. A total of  $2 \times 10^4$  cells/well were seeded in a Transwell cell chamber, and serum-free DMEM medium was added to the lower chamber. After culturing for 24 h, the liquid in the lower chamber was collected and centrifuged at 800 g for 5 min, and the cells were collected and counted. The cells in the Transwell cell were erased, fixed with 4% paraformaldehyde solution at room temperature for 60 min, and stained with 0.5% crystal violet. The number of cells that passed through the mold was counted under a light microscope, and the cell migration inhibition rate was calculated as follows: (the number of cells in the control group – the number of cells in the experimental group) / the number of cells in the control group. The experiment was repeated three times.

#### Immunofluorescence assay

Briefly,  $2 \times 10^5$  cells/well A2780/DDP were seeded on slides in 6-well plates. After 16 h of adherence, cells were incubated in different groups (blank control group: final concentration cisplatin 0  $\mu\text{g}/\text{mL}$  + GFC 0  $\text{mg}/\text{mL}$ , cisplatin single-action group: final concentration 3.743  $\mu\text{g}/\text{mL}$ , GFC single-action group: final concentration 0.063  $\text{mg}/\text{mL}$ , and drug combination group: final concentration cisplatin 3.743  $\mu\text{g}/\text{mL}$  + GFC 0.063  $\text{mg}/\text{mL}$ ), cultured them for 24 h. The slides were fixed in 4% paraformaldehyde for 15 min after washing with PBS, and then permeabilized with 0.5% Triton X-100 for another 15 min. A 5% BSA solution was added dropwise to the slide and blocked for 1 h at room temperature. Primary antibodies were added dropfold and incubated overnight at 4  $^{\circ}\text{C}$ . Cy3-labeled fluorescent secondary antibody was added and incubated for 1 h. The experiment was repeated three times, and the images were observed and collected under a fluorescence microscope.

#### Cell pseudopodia fluorescence assay

Briefly,  $2 \times 10^5$  cells/well A2780 cells and A2780/DDP were seeded in 6-well plates. After 16 h of adherence, cells were incubated in different groups (blank control group: final concentration cisplatin 0  $\mu\text{g}/\text{mL}$  + GFC 0  $\text{mg}/\text{mL}$ , cisplatin single-action group: final concentration 3.743  $\mu\text{g}/\text{mL}$ , GFC single-action group: final concentration 0.063  $\text{mg}/\text{mL}$ , and drug combination group: final concentration cisplatin 3.743  $\mu\text{g}/\text{mL}$  + GFC 0.063  $\text{mg}/\text{mL}$ ), cultured them for 24 h. After the coverslips of the climbed cells were washed with PBS, the climbs were fixed with 3.7% paraformaldehyde for 20 min, after which the cells were washed with 0.1% Triton X-100 for 3 times for 5 min each. A dilution ratio of 1:40 was added the cells were incubated with Actin-Tracker Green (Beyotime Biotechnology, China) for 60 min at room temperature in the dark. The experiment was repeated three times, and the images were observed and collected under a fluorescence microscope.

#### Cell autophagy was detected by fluorescence

Briefly,  $2 \times 10^5$  cells/well A2780 cells and A2780/DDP were seeded in 6-well plates. After 16 h of adherence, cells were incubated in different groups (blank control group: final concentration cisplatin 0  $\mu\text{g}/\text{mL}$  + GFC 0  $\text{mg}/\text{mL}$ , cisplatin single-action group: final concentration 3.743  $\mu\text{g}/\text{mL}$ , GFC single-action group: final concentration 0.063  $\text{mg}/\text{mL}$ , and drug combination group: final concentration cisplatin 3.743  $\mu\text{g}/\text{mL}$  + GFC 0.063  $\text{mg}/\text{mL}$ ), cultured them for 24 h. The cells were washed once with PBS, then 1ml MDC staining solution (Beyotime Biotechnology, China) was added and incubated at 37  $^{\circ}\text{C}$  in the dark for 30min. The experiment was repeated three times, and the green fluorescence was observed under a fluorescence microscope.

mL + GFC 0.063  $\text{mg}/\text{mL}$ ), cultured them for 24 h. The cells were washed once with PBS, then 1ml MDC staining solution (Beyotime Biotechnology, China) was added and incubated at 37  $^{\circ}\text{C}$  in the dark for 30min. The experiment was repeated three times, and the green fluorescence was observed under a fluorescence microscope.

#### Cell autophagy was detected by transmission electron microscopy

Briefly,  $2 \times 10^5$  cells/well A2780 cells and A2780/DDP were seeded in 6-well plates. After 16 h of adherence, cells were incubated in different groups (blank control group: final concentration cisplatin 0  $\mu\text{g}/\text{mL}$  + GFC 0  $\text{mg}/\text{mL}$ , cisplatin single-action group: final concentration 3.743  $\mu\text{g}/\text{mL}$ , GFC single-action group: final concentration 0.063  $\text{mg}/\text{mL}$ , and drug combination group: final concentration cisplatin 3.743  $\mu\text{g}/\text{mL}$  + GFC 0.063  $\text{mg}/\text{mL}$ ), cultured them for 24 h. The cells were washed once with PBS, and the cells were collected after trypsin digestion. 2.5% glutaraldehyde was added sequentially overnight, followed by fixation with hungry acid fixative for 2 h, gradient dehydration with acetone solution, and embedding of samples. The sections were stained with uranyl acetate for 30min, followed by lead citrate for 15min. The experiment was repeated three times, the autophagy was observed by transmission electron microscope.

#### In vivo experiments

Creating a xenograft rat model of ovarian cancer, twenty female BALB/c nude mice weighing (20 $\pm$ 2)g were subcutaneously injected with 0.2ml of A2780/DDP cells ( $1 \times 10^7$  cells/mL) into the right flank. The mice were randomly divided into four groups with five mice in each group. The body weight, food intake, tumor size and activity status of the mice were recorded daily, once the tumor had grown to a size of 50–100  $\text{mm}^3$ . Control group (received an equal volume of saline orally), cisplatin alone group, GFC alone group, and cisplatin + GFC combination group. Cisplatin was administered by intraperitoneal injection twice a week at a dose of 2mg/kg, and GFC was administered daily by gavage at a dose of 20 g/kg according to the dose of human and mouse administration. Tumor size was measured every two days to evaluate the effect of drug treatment. Their care during research on animals follows ARRIVE guidelines and is conducted in accordance with the National Institutes of Health Guidelines for the Care and Use of Laboratory Animals (NIH Publication No. 8023, as revised in 1978). After 14 days, the tumor tissues of the mice were stained with HE and the protein expression levels were detected by western blot.

#### Plasmid constructs and transfection

Recombinant plasmid pcDNA3.1(+)-EGFP-PA2G4 and pcDNA3.1(+)-EGFP-Mock were constructed by OBiO Technology Co. Ltd (Shanghai, China). A total of  $2 \times 10^5$  cells were seeded on 6-well plates and cultured for 18 h. pcDNA3.1(+)-EGFP-PA2G4 or pcDNA3.1(+)-EGFP-Mock was transfected into the cells with GoldenTran DR Reagent (Golden Trans Technology Co., Ltd., Changchun, China). Primers were synthesized by OBiO Technology Co. Ltd (Shanghai, China) to amplify the whole DNA fragment of PA2G4. The sequences were 5'-CAGGAGCAAACACTATCGCTGAG-3' and 5'-GGACCGAAGTACCCTGTTGG-3' for forward primer and reverse primer, respectively.

#### Quantitative real-time PCR (qRT-PCR)

RNA was isolated with RNA-easy Isolation Reagent (Vazyme, China), and cDNA was reverse-transcribed by HiScript II Q Select RT SuperMix for qPCR Kit (Vazyme, China) at 37  $^{\circ}\text{C}$  for 15 min, and at 85  $^{\circ}\text{C}$  for 5 s. The expression of the target gene was quantitated by using ChamQ Universal SYBR qPCR Master Mix (Vazyme, China), and was performed in duplicates using the following conditions: 95  $^{\circ}\text{C}$  for 30 s, followed by 40 cycles of 95  $^{\circ}\text{C}$  for 10 s, and 60  $^{\circ}\text{C}$  for 30 s. Water was used instead of

the DNA template as a negative sample control, and DNA provided within the kit was used as a positive sample control.  $\beta$ -Actin gene was used as an internal control. The experiment was repeated three times, relative mRNA expression was calculated using the formula  $2^{-\Delta\Delta Ct}$ .

#### Western blot

RIPA Lysis buffer was used to isolate all of the cellular proteins (Beyotime, China). After centrifuging the cell lysate at 13,000 g for 5 min, the supernatant was collected and refrigerated at 80 °C. To guarantee a constant protein content in each sample, protein concentrations were determined using the BCA Protein Assay Kit (Solarbio, China). The protein extract was then added to each well in amounts of 20 or 25, electrophoretically separated on a 10% SDS-polyacrylamide gel, and then transferred to a polyvinylidene fluoride membrane (Millipore) at 300 mA for two hours. The membrane was first incubated with the primary antibody for 1 h at room temperature after being blocked with skimmed milk for 2 hours. The fluorescently tagged secondary antibodies were incubated with the membrane for 30 minutes at room temperature and detected using Two-color Infrared Laser Imaging System (Odyssey, U.S.). No cell lysates were used as negative sample controls. The expression of  $\beta$ -actin was used as the internal control. The experiment was repeated three times, and Image J calculated the gray value of protein bands.

#### Chemical constituents of GFC based on LC-MS/MS analysis

The GFC powder was dissolved in 50% aqueous methanol, and the supernatant was retained after centrifugation. Using Q Exactive Orbitrap high resolution mass spectrometry to mass spectrum data collection, specific parameters setting is: The positive ion and negative ion modes were scanned separately. The ion source voltage was 3.2kV, Capillary temp was 320 °C, Aux gas heater temp was 350 °C, Sheath gas flow rate was 40L/min. The Aux gas flow rate was 15L/min.

#### Statistical analyses

The data are given as mean $\pm$ SD since each experiment was carried out three times. A two-tailed Student's *t* test was used to assess the differences between the two groups. Analysis of variance (ANOVA) was used to assess the differences between multiple sets of data. *P* value lower than 0.05 was considered significant. Data were analyzed using SPSS 17.0.

## Results

#### PA2G4 gene expression in clinical normal tissues and tumors

The expression of PA2G4 gene is significantly higher in many tumor tissues, but there is no significant difference in expression levels in ovarian tumors (Fig. 1-A and Fig. 1-B). The PA2G4 gene has no significant effect on the survival rate of ovarian tumor patients (Fig. 1-C). However, the expression level of PA2G4 gene in grade 3 ovarian tumors was significantly higher than that in grade 2 ovarian tumors ( $P < 0.01$ ) (Fig. 1-D and Fig. 1-E).

#### A2780 cells and A2780/DDP cells show differences in cell cisplatin resistance and migration invasion

As shown in Fig. 2-A, A2780 and A2780/DDP cell exhibited a negative trend as cisplatin concentration was raised. A2780 cells and A2780/DDP cells have  $IC_{50}$  values for cisplatin of 9.44  $\mu$ g/mL and 21.85  $\mu$ g/mL (Fold change=1.25), respectively. In addition, compared with A2780 cells, the invasion and migration ability of A2780/DDP cells was significantly increased (Invasion: Fold change=0.73, Migration: Fold change=1.09) (Fig. 2-B and Fig. 2-C). We observed through fluorescence

microscopy that the pseudopodial cell elongation of A2780/DDP cells was significantly higher than that of A2780 cells (Fig. 2-D and Fig. 2-E). The expression of adhesive-related protein N-cadherin was significantly increased (Fold change=1.06) and E-cadherin was significantly decreased (Fold change=0.23) in A2780/DDP cells compared with A2780 cells; and the expression of  $\alpha$ -Actin, the microfilament protein that makes up the pseudopodia, was significantly increased (Fold change=0.46) (Fig. 2-F).

#### GFC chemical composition identification

In the positive ion mode and the negative ion mode TIC scanning figures, as shown in Fig. 3-A and Fig. 3-B respectively, characteristic peaks were identified by comparing with the mzCloud and mzVault TCM natural product databases. Based on the arrangement of chemical component relative content, the top ten chemical constituents were Paeonol (27.407%), Paeoniflorin (12.662%), Amygdalin (10.778%), 1,2,3,4,6-Pentagalloylglucose (6.499%), Gallic acid (6.369%), Benzoylpaeoniflorin (4.868%), Ethyl gallate (4.733%), Albiflorin (3.575%), Pachymic acid (2.921%) and Pyrogallol (2.869%). Detailed chemical information is shown in Table 1.

#### GFC combined with cisplatin inhibits A2780/DDP cell invasion and migration

A2780/DDP cell growth was directly inhibited by GFC (Fig. 4-A). The combination of GFC (0.063 mg/mL, equal to  $IC_{50}$  value) and cisplatin (3.743  $\mu$ g/mL, equal to  $IC_{50}$  value) has no statistically significant effect on cell proliferation activity (Fig. 4-B), but it can significantly inhibit the invasion and migration of A2780/DDP cells (Invasion: Fold change=1.50, Migration: Fold change=1.66) (Fig. 4-C and Fig. 4-D). The number of filopodia and lamellipodia of A2780/DDP cells in the combined treatment group was significantly inhibited (Fig. 4-E and Fig. 4-F). Western blot results showed that A2780/DDP cells in the combined treatment group significantly inhibited the expression of adhesion-related proteins, N-cadherin (Fold change=1.32), matrix metalloproteinase-2 (MMP-2) (Fold change=1.29), and Vimentin (Fold change=1.15); significantly decreased the expression levels of Snail (Fold change=1.14) and Slug proteins (Fold change=1.81); and significantly increased the expression levels of E-cadherin (Fold change=1.02) (Fig. 4-G). The expressions of LIMK1 (Fold change=1.14), Cofilin (Fold change=1.29) and  $\alpha$ -Actin (Fold change=1.32) in A2780/DDP cells were significantly decreased in the combination group (Fig. 4-H).

#### GFC combined with cisplatin targeted PA2G4 gene to inhibit PI3K/AKT/GSK-3 $\beta$ signaling pathway in A2780/DDP cells

The PA2G4 gene is highly expressed in A2780/DDP cells (Fold change=2.32) (Fig. 5-A). GFC combined with cisplatin inhibits p-PI3K in A2780/DDP cells. As shown in the Fig. 5-B to D, GFC combined with cisplatin inhibited the expression levels of p-PI3K (Fold change=1.81), p-AKT (Fold change=1.83) and p-GSK-3 $\beta$  (Fold change=0.94) in A2780/DDP cells, and also inhibited the expression of PA2G4 (Fold change=0.22) mRNA in the cells.

To investigate the regulatory role of GFC on PA2G4 in inhibiting the PI3K/AKT/GSK-3 $\beta$  signaling pathway, we constructed Over-NC and Over-PA2G4 vectors for cell transfection. As shown in Fig. 5-D, compared with the Over-NC group, the Over-NC+combined drug group could significantly inhibit the protein expression levels of p-PI3K, p-AKT and p-GSK-3 $\beta$ . There was no significant difference in the protein expression of p-PI3K, p-AKT and p-GSK-3 $\beta$  between Over-NC group and Over-PA2G4 group without drug intervention. Compared with the Over-PA2G4 group, the Over-PA2G4+combined with drug group could significantly inhibit the protein expression levels of p-PI3K, p-AKT and p-GSK-3 $\beta$ . The same experiments were grouped to study cell invasion

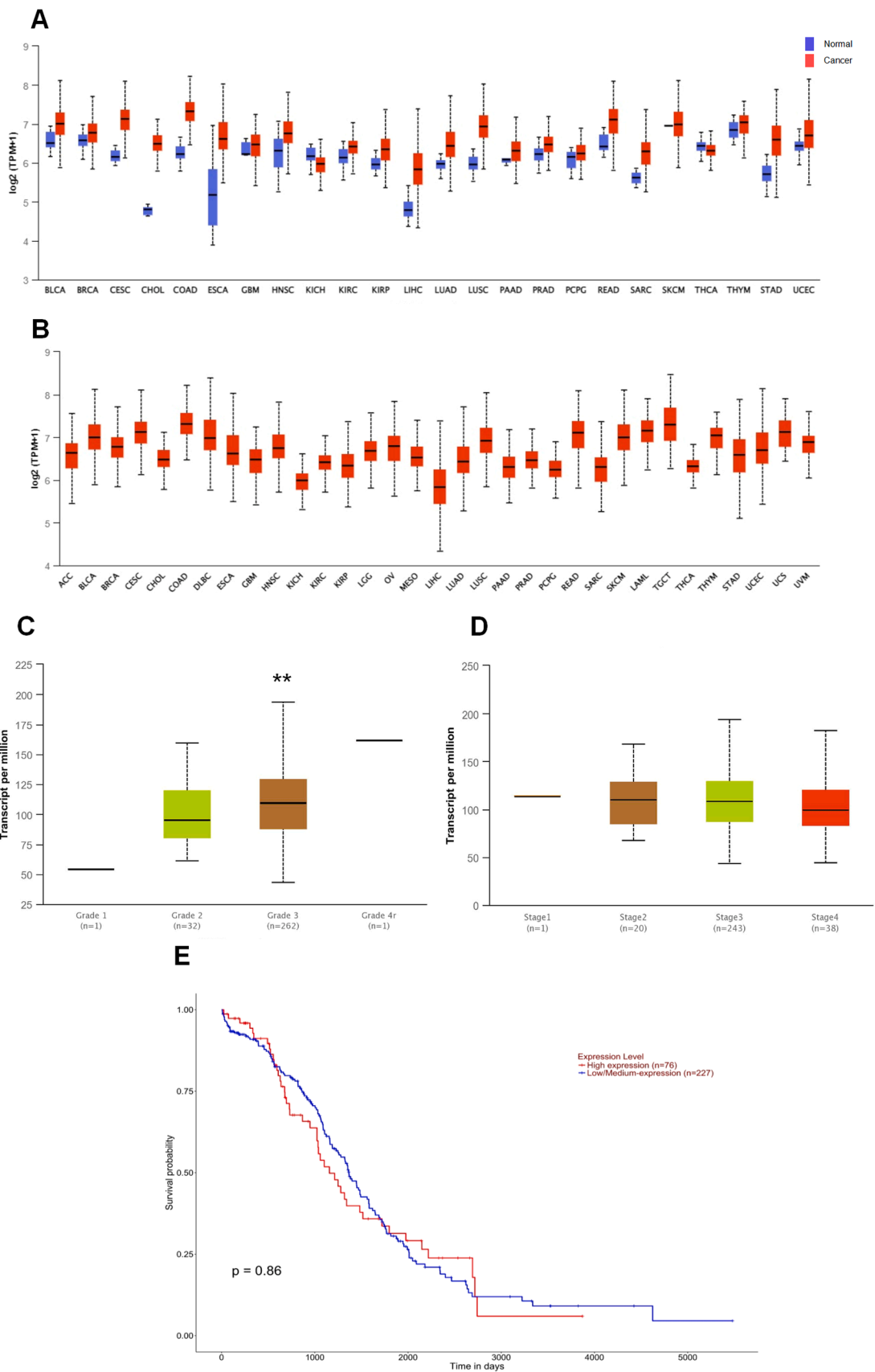
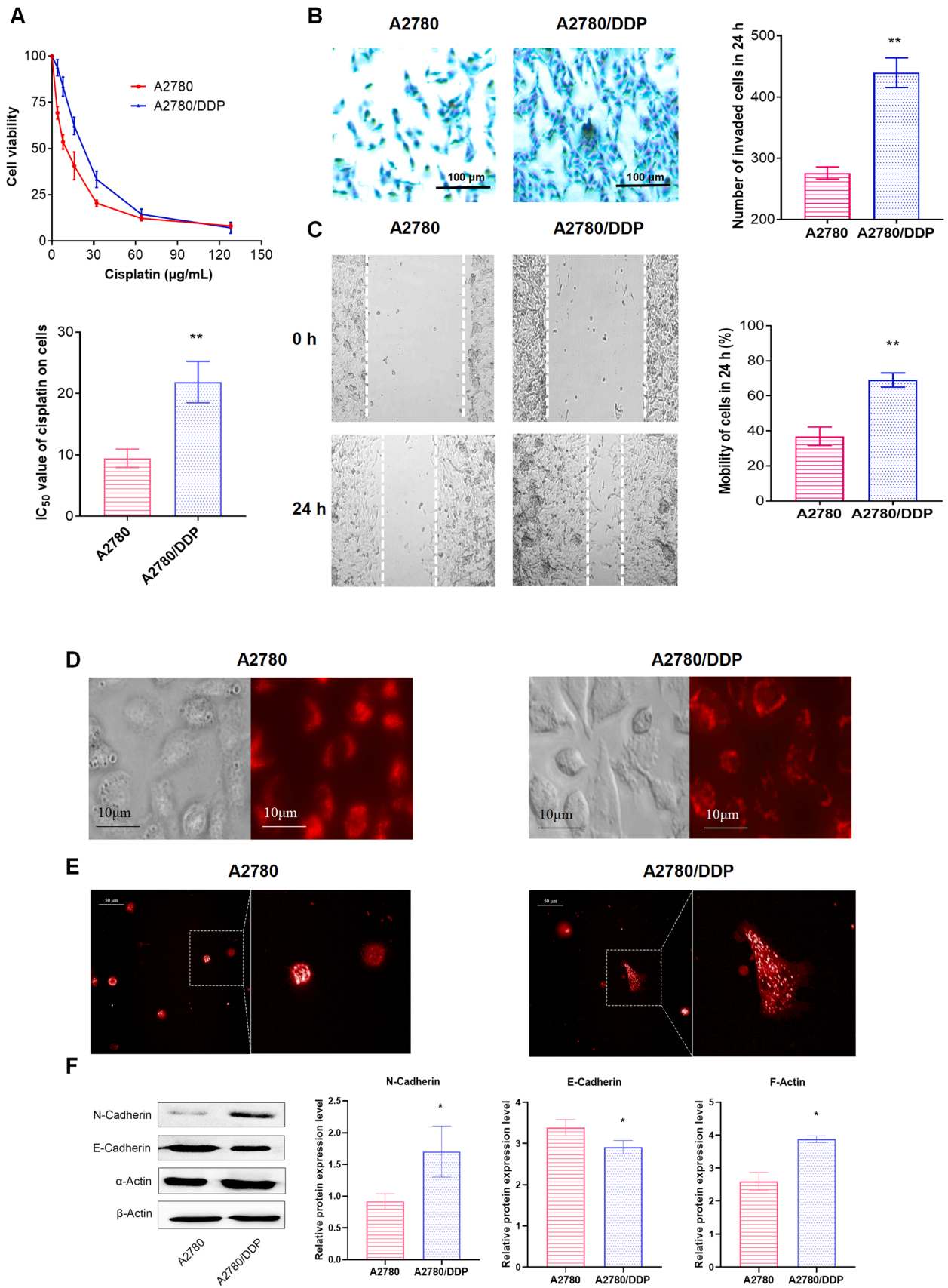


**Fig. 1.** Expression of PA2G4 gene in patients and its effect on their survival. Expression of PA2G4 gene in various normal tissues and cancers (A); expression in cancer (B); expression in ovarian tumors of different grades (C); expression in progressive ovarian cancer (D); survival curve (E). Clinical data obtained from <http://ualcan.path.uab.edu/>.



(caption on next page)

**Fig. 2.** Differences in biological characteristics between ovarian cancer cisplatin-sensitive A2780 cells and cisplatin-resistant A2780/DDP cells. The morphology of A2780 cells and A2780/DDP cells was observed by light microscopy (A and B). The effects of different concentrations of cisplatin on the cell viability of A2780 cells and A2780/DDP cells were detected by CCK-8 method; comparison of IC<sub>50</sub> values of cisplatin on A2780 cells and A2780/DDP cells (A). The invasion ability of A2780 cells and A2780/DDP cells was detected by Transwell method (B). The migration ability of A2780 cells and A2780/DDP cells was detected by scratch assay (C). Intercellular adhesion was detected by immunofluorescence (D). Cellular pseudopodia was detected by laser confocal method (E). Western blot detection of adhesion and pseudopod-related regulatory proteins expression in A2780 cells and A2780/DDP cells (F). The experiments were repeated three times, and the results are expressed as the mean ± standard deviation, with β-actin as the internal reference. ImageJ software statistics protein gray value, cell invasion number and cell migration rate, and GraphPad Prism 8 was used for statistical analysis of the data. Neurogenic cadherin, N-Cadherin; Epithelial cadherin, E-cadherin; α-Smooth Muscle Actin, α-Actin .

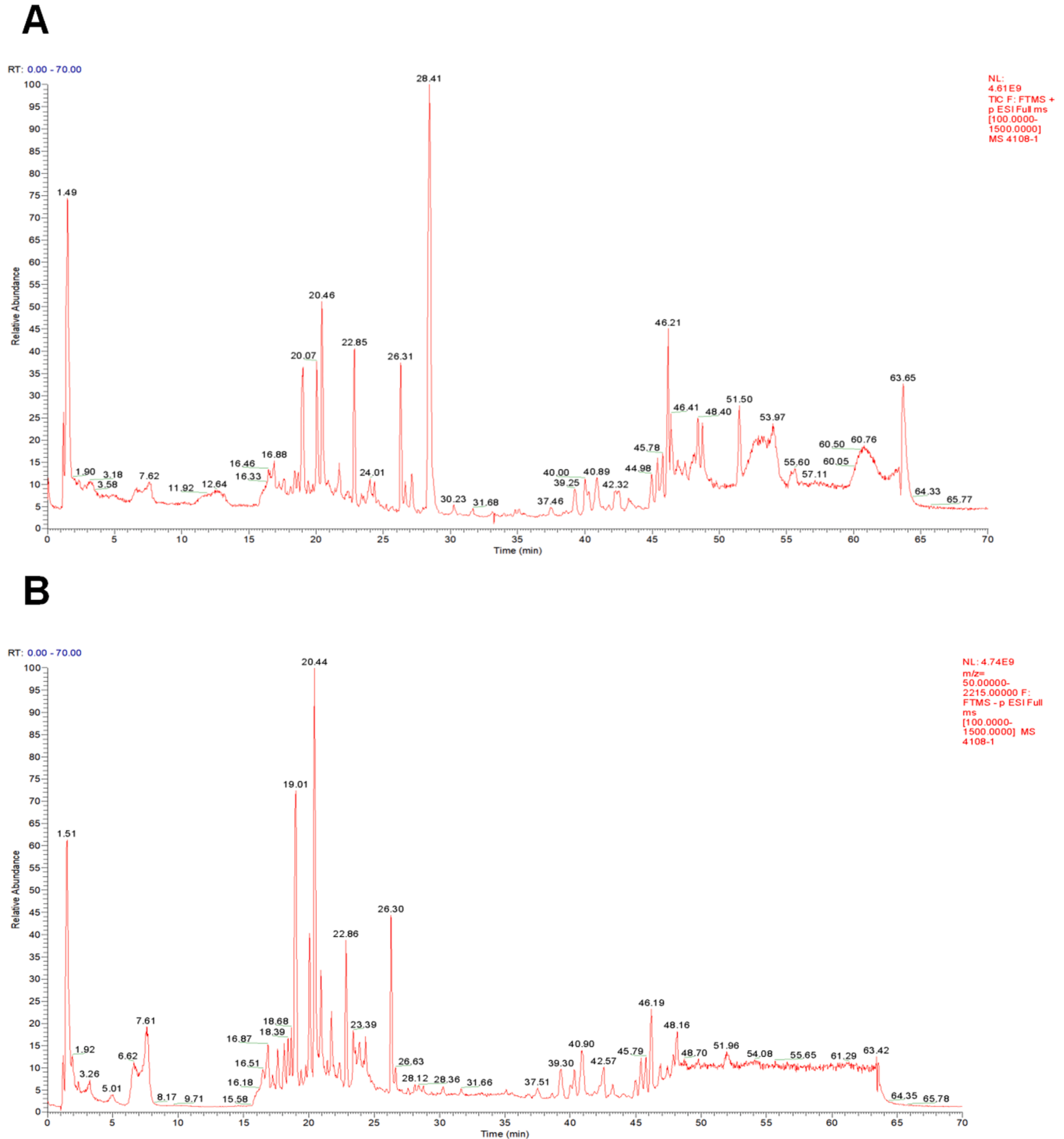


**Fig. 3.** Total ion current diagram of GFC extraction solution, in the positive ions and negative ions detection mode.

**Table 1**  
Information of GFC compounds identified.

Name	Molecular formula	Mass deviation (ppm)	Molecular weight	Retention time (min)	Match score	Peak area	Relative content (%)
Paeonol	C9 H10 O3	-0.48	166.06292	28.429	94.8	53,908,929,641	27.407
Paeoniflorin	C23 H28 O11	-1.11	480.16263	20.433	93.4	24,906,338,505	12.662
Amygdalin	C20 H27 N O11	-0.77	457.15806	18.992	92.9	21,199,997,662	10.778
1,2,3,4,6-Pentagalloylglucose	C41 H32 O26	-0.9	940.11733	23.663	91.2	12,783,018,795	6.499
Gallic acid	C7 H6 O5	-0.96	170.02136	7.592	93	12,526,931,321	6.369
Benzoylpaeoniflorin	C30 H32 O12	-0.97	584.18881	26.284	95	9,574,903,567	4.868
Ethyl gallate	C9 H10 O5	-1.05	198.05262	20.925	91.6	9,309,563,027	4.733
Albiflorin	C23 H28 O11	-0.9	480.16273	20.061	90.1	7,032,316,615	3.575
Pachymic acid	C33 H52 O5	-0.84	528.38103	46.18	81.1	5,744,890,835	2.921
Pyrogallol	C6 H6 O3	-1.84	126.03146	7.642	84.1	5,643,467,811	2.869
Citric acid	C6 H8 O7	-0.53	192.0269	1.649	91.8	4,194,412,793	2.132
Oxypaeoniflorin	C23 H28 O12	-0.68	496.15774	18.663	92.9	3,900,288,374	1.983
Cinnamaldehyde	C9 H8 O	-0.29	132.05748	27.128	91.4	2,877,045,167	1.463
3-O-Acetyl-1 $\alpha$ -hydroxytrametenolic acid	C32 H50 O5	-0.94	514.36534	45.386	82.3	2,496,554,185	1.269
Sucrose	C12 H22 O11	-0.68	342.11598	1.526	94.7	2,365,455,205	1.203
Coumarin	C9 H6 O2	-0.76	146.03667	24.025	86.9	2,202,108,618	1.120
Dehydrotumulosic acid	C31 H48 O4	-0.73	484.35491	40.318	74.6	2,193,227,732	1.115
Cantharidin	C10 H12 O4	-1.14	196.07334	22.849	77	1,871,585,983	0.952
Poricoic acid A	C31 H46 O5	-0.44	498.3343	40.805	90.9	1,797,810,281	0.914
Ellagic acid	C14 H6 O8	-1.31	302.00587	21.769	86.8	1,041,117,568	0.529
6-Hydroxyindole	C8 H7 N O	-0.09	133.05275	11.987	71.2	807,708,626.1	0.411
Betaine	C5 H11 N O2	0.22	117.079	1.511	85.3	799,375,491.5	0.406
Xanthoxylone	C10 H12 O4	-1.22	196.07332	20.062	80.2	666,821,866.4	0.339
Wilforlide A	C30 H46 O3	-0.43	454.3445	39.194	77	598,573,726.3	0.304
Paeonolide	C20 H28 O12	-0.31	460.15793	19.761	78.7	539,736,990.6	0.274
Protocatechualdehyde	C7 H6 O3	-1.47	138.03149	17.818	84	432,493,005.2	0.220
(+)-Magnoflorine	C20 H23 N O4	-0.29	341.16261	20.236	88	406,690,031.9	0.207
Manninotriose	C18 H32 O16	-0.31	504.16888	1.526	78.5	393,368,739.7	0.200
4-Hydroxybenzoic acid	C7 H6 O3	-1.57	138.03148	18.179	82.7	362,262,261	0.184
Nicotinic acid	C6 H5 N O2	0.26	123.03206	2.603	76.9	355,350,564.3	0.181
Alisol B	C30 H48 O4	-0.84	494.33941	44.914	87.2	355,052,804.1	0.181
Boldine	C19 H21 N O4	-0.77	327.14681	19.99	78.8	318,208,932.3	0.162
Protocatechuic acid	C7 H6 O4	-1.18	154.02643	16.034	84.4	311,358,288.5	0.158
Ferulaldehyde	C10 H10 O3	-0.92	178.06283	18.664	72.3	302,593,603.3	0.154
$\alpha$ -Linolenic acid	C18 H30 O2	-0.61	278.22441	47.037	82.2	212,159,104.6	0.108
Azelaic acid	C9 H16 O4	-1.13	188.10465	22.938	73.4	207,961,703.6	0.106
Uridine	C9 H12 N2 O6	0.42	244.06964	5.247	89.2	138,925,417.1	0.071
5-Hydroxy-1-tetralone	C10 H10 O2	-0.41	162.06801	28.96	81.9	133,982,098.5	0.068
Androsin	C15 H20 O8	-0.71	328.11558	19.789	71.1	117,039,880.5	0.060
Oleanonic acid	C30 H46 O3	-0.49	454.34447	50.978	82.4	116,498,404.9	0.059
Abscisic acid	C15 H20 O4	-0.8	264.13595	24.663	73.9	108,340,388.8	0.055
Naringenin chalcone	C15 H12 O5	-0.63	272.0683	26.931	87.4	98,571,163.88	0.050
Ethyl 3,4-dihydroxybenzoate	C9 H10 O4	-0.86	182.05775	23.439	80	89,794,984.45	0.046
(-)-Epicatechin gallate	C22 H18 O10	-0.5	442.08977	21.445	83.2	87,551,275.7	0.045
Methyl hexadecanoate	C17 H34 O2	-0.84	316.26097	37.562	78.1	86,842,383.36	0.044
Methyl gallate	C8 H8 O5	-1.6	184.03688	18.595	86.2	80,908,135.93	0.041
Benzoic acid	C7 H6 O2	-1.57	122.03659	21.435	83.2	70,693,911.23	0.036
Gentisic acid	C7 H6 O4	-1.18	154.02643	18.182	81.7	69,672,126.53	0.035
Morin	C15 H10 O7	-0.75	302.04243	25.495	80	66,199,353.44	0.034
Corilagin	C27 H22 O18	0.14	634.0807	17.832	81.7	57,458,651.37	0.029
Dehydrotrametenolic acid	C30 H46 O3	-0.51	454.34446	42.416	78.6	55,436,568.03	0.028
Kahweol	C20 H26 O3	-0.51	314.18804	38.376	73.8	51,893,311.34	0.026
Eupatilin	C18 H16 O7	-0.23	344.08953	33.964	70.6	50,183,721.95	0.026
3,5-Dimethoxy-4-hydroxybenzaldehyde	C9 H10 O4	-0.17	182.05788	21.372	84.9	43,803,622.75	0.022
Norisoboldine	C18 H19 N O4	-1.31	313.131	19.6	71.2	41,648,996.11	0.021
Quercetin 7-rhamnoside	C21 H20 O11	-0.18	448.10048	22.614	76.9	40,790,098.15	0.021
Methyl 4-hydroxy-3-methoxycinnamate	C11 H12 O4	-0.44	208.07347	23.058	73.6	35,684,638.88	0.018
Sweroside	C16 H22 O9	-2.19	358.1256	22.856	72.1	35,606,517.88	0.018
(+)-Catechin hydrate	C15 H14 O6	0.07	290.07906	17.993	72.7	35,114,051.12	0.018
Bryodulcosigenin	C30 H50 O4	-0.49	496.35521	44.516	76.3	34,579,494.11	0.018
Naringenin	C15 H12 O5	-1.03	272.06819	21.391	75	33,612,631.34	0.017
Stachyose	C24 H42 O21	0.37	666.22211	2.354	87.8	27,316,326.45	0.014
Baicalin	C21 H18 O11	-0.74	446.08458	23.735	77.7	24,311,562.36	0.012
Rosarin	C20 H28 O10	-1.31	445.19451	21.379	79.8	24,084,399.88	0.012
Maltopentaose	C30 H52 O26	0.46	828.27506	2.52	92.1	23,535,441.54	0.012
Abietic Acid	C20 H30 O2	-0.96	302.22429	40.489	81	21,093,910.27	0.011
Shikimic acid	C7 H10 O5	-1.31	174.0526	2.215	80.6	20,242,949.15	0.010
18 $\beta$ -Glycyrrhetic Acid	C30 H46 O4	0.35	470.33978	39.901	76.7	19,584,351.17	0.010
Wogonin	C16 H12 O5	-0.45	284.06835	31.546	74.5	18,066,250.76	0.009

(continued on next page)

Table 1 (continued)

Name	Molecular formula	Mass deviation (ppm)	Molecular weight	Retention time (min)	Match score	Peak area	Relative content (%)
Curcumenol	C15 H22 O2	-0.74	234.16181	29.807	82.3	16,084,692.89	0.008
Phloridzin	C21 H24 O10	-0.79	436.1366	23.091	81	14,762,756.54	0.008
Curculigoside	C22 H26 O11	-0.47	466.14729	20.245	81.3	11,548,177.47	0.006
Ligustilide	C12 H14 O2	-0.39	190.09931	36.07	73.3	10,490,963.01	0.005
Dehydrocostus lactone	C15 H18 O2	-0.74	230.13051	25.587	74.9	10,216,630.67	0.005
Dehydrodiisoeugenol	C20 H22 O4	-0.74	326.15157	25.791	77	9,960,009.423	0.005
Diammonium glycyrrhizinate	C42 H62 O16	0.4	822.40412	29.786	88	8,976,420.402	0.005
2'-O-Galloylhyperin	C28 H24 O16	-0.8	616.10594	23.697	76.7	7,442,558.315	0.004
Isolantalactone	C15 H20 O2	-0.44	232.14623	27.851	70.7	6,914,820.027	0.004

and migration and their regulatory protein expression levels. Compared with the Over-NC group, the Over-NC+drug group could significantly inhibit the cell invasion and migration. There was no significant difference in invasion and migration between Over-NC group and Over-PA2G4 group without drug intervention. Compared with the Over-PA2G4 group, the Over-PA2G4+ drug group could significantly inhibit the cell invasion and migration (Fig. 5-E to J).

#### Anti-tumor effect of GFC combined with cisplatin in vivo

To evaluate the anti-tumor effect of GFC combined with cisplatin in tumor-bearing mice, a xenograft A2780/DDP tumor mouse model was established. As shown in the Fig. 6-A, compared with the model group, the tumor volume of the combined drug group was significantly reduced from day 8 ( $P < 0.05$ ). The results of HE staining showed that the density of tumor tissue, the degree of cell arrangement disorder, the number of cells and nuclear atypia were decreased after the combined treatment (Fig. 6-B). These results indicate that GFC combined with cisplatin can inhibit tumor growth in vivo. In order to further study the effect of GFC combined with cisplatin on the tumor tissue of A2780/DDP cells, WB quantitative analysis showed that GFC combined with cisplatin could inhibit the expression of EMT-related proteins N-Cadherin (Fold change=1.73), MMP-2 (Fold change=0.15), Vimentin (Fold change=0.29), Snail (Fold change=1.71) and Slug (Fold change=1.86). It promoted E-Cadherin protein expression (Fold change=1.58) (Fig. 6-C).

#### Discussion

With the advancement of modern science, more treatment options are becoming available for cancer, including surgery, chemotherapy, radiotherapy, biological therapy, targeted therapy, and immunotherapy [29–31]. However, the treatment of advanced cancer patients is still a combination of surgery, radiotherapy, and chemotherapy, which not only shrinks tumors and improves clinical symptoms, but also improves the quality of life of patients with advanced cancer [32,33]. Platinum drugs are important chemotherapeutic drugs. They are widely used in the clinical treatment of various types of tumors, especially lung cancer, ovarian cancer, and colon cancer, and they can inhibit tumor recurrence and metastasis [34,35]. However, tumors often develop resistance to chemotherapy drugs, resulting in the failure of chemotherapy and causing great pain to patients [36,37].

Epithelial-mesenchymal transition (EMT) refers to the process where epithelial cells undergo a series of biochemical changes to become mesenchymal cells with invasive ability [38,39]. Activation of EMT is a key process in cancer cell metastasis, during which epithelial cells acquire mesenchymal characteristics with enhanced cell motility and migratory capacity [40]. EMT is divided into the following three categories: type I, type II, and type III [41]. Unlike types I and II, which are necessary for physiological functions, type III is a pathophysiological adaptation of the process, which is related to tumorigenesis. Certain epigenetic and genetic changes are closely related to progression in cells

[42,43]. After EMT changes, tumor cells can invade the tissues around the primary tumor, exude lymphatic or blood vessels, reach distant sites through circulation, and eventually colonize metastatic sites [44]. EMT is the sum of multiple processes with common features, manifested by the dissolution of intercellular junctions such as cytokeratin and E-cadherin, cytoskeletal rearrangements such as loss of the typical polygonal or fusiform fibrocyte-like appearance and elevation of mesenchymal cell markers such as N-Cadherin [45]. In this study, ovarian cancer cisplatin-sensitive cell line A2780 and cisplatin-resistant cell line A2780/DDP were used to investigate the relationship between EMT and cisplatin resistance. Compared with A2780 cells, A2780/DDP cells showed increased invasion and migration, decreased intercellular adhesion, and increased pseudopod formation. The results of western blot showed that the expression levels of N-cadherin and  $\alpha$ -Actin were significantly higher in A2780/DDP cells compared with A2780 cells, and the expression level of E-cadherin was significantly lower. These data suggest that elevated EMT levels in the ovarian cancer cisplatin-resistant cell line A2780/DDP are closely associated with the cisplatin-resistant phenotype. Further analysis by immunofluorescence and laser confocal method showed that the adhesion of A2780/DDP cells was significantly decreased and the formation of pseudopodia was significantly increased compared with A2780 cells.

Phosphatidylinositol 3-kinase (PI3K) has serine/threonine (Ser/Thr) kinase and phosphatidylinositol kinase activities, which are involved in the regulation of various cellular functions such as proliferation, differentiation, and glucose transport [46]. Akt is a serine/threonine-specific protein kinase that plays an important role in cell survival and apoptosis [47]. Abnormal activity of the PI3K/AKT signaling pathway is found in various human tumors, which is closely related to the occurrence and development of tumor cells [48–51]. It has been shown that inhibiting the PI3K/AKT signaling pathway can inhibit the EMT and promote NF- $\kappa$ B-mediated apoptosis in lung adenocarcinoma A549 cells, and reverse their resistance to cisplatin [52]. It has been found that the expression of Foxo-1 is decreased in platinum-resistant ovarian cancer, and Foxo-1 is negatively regulated by the PI3K/AKT signaling pathway. By inhibiting the PI3K/AKT signaling pathway, the expression of Foxo-1 could be induced to reduce the occurrence of drug resistance in ovarian cancer [53]. Glycogen synthase kinase 3 $\beta$  (GSK-3 $\beta$ ) is an evolutionarily conserved serine/threonine kinase that acts on numerous signaling proteins, structural proteins, and transcription factors to regulate cell differentiation, proliferation, survival, and apoptosis [54]. According to Liu et al., Transgelin 2 directly interacts with PTEN, activates the PI3K/AKT/GSK-3 $\beta$  signaling pathway, and promotes taxol resistance as well as metastasis and invasion of breast cancer [55]. Wei et al. found that the increased expression of the PI3K/Akt/GSK-3 $\beta$ / $\beta$ -catenin signaling pathway in prostate cancer PC-3 and DU145 cells promoted cell proliferation, growth, migration, and invasion [56]. However, the expression and function of PI3K/AKT/GSK-3 $\beta$  in ovarian cancer and the underlying mechanisms remain largely unknown.

Traditional Chinese medicine has been applied for thousands of years. At present, Chinese medicine is a very important discipline in the

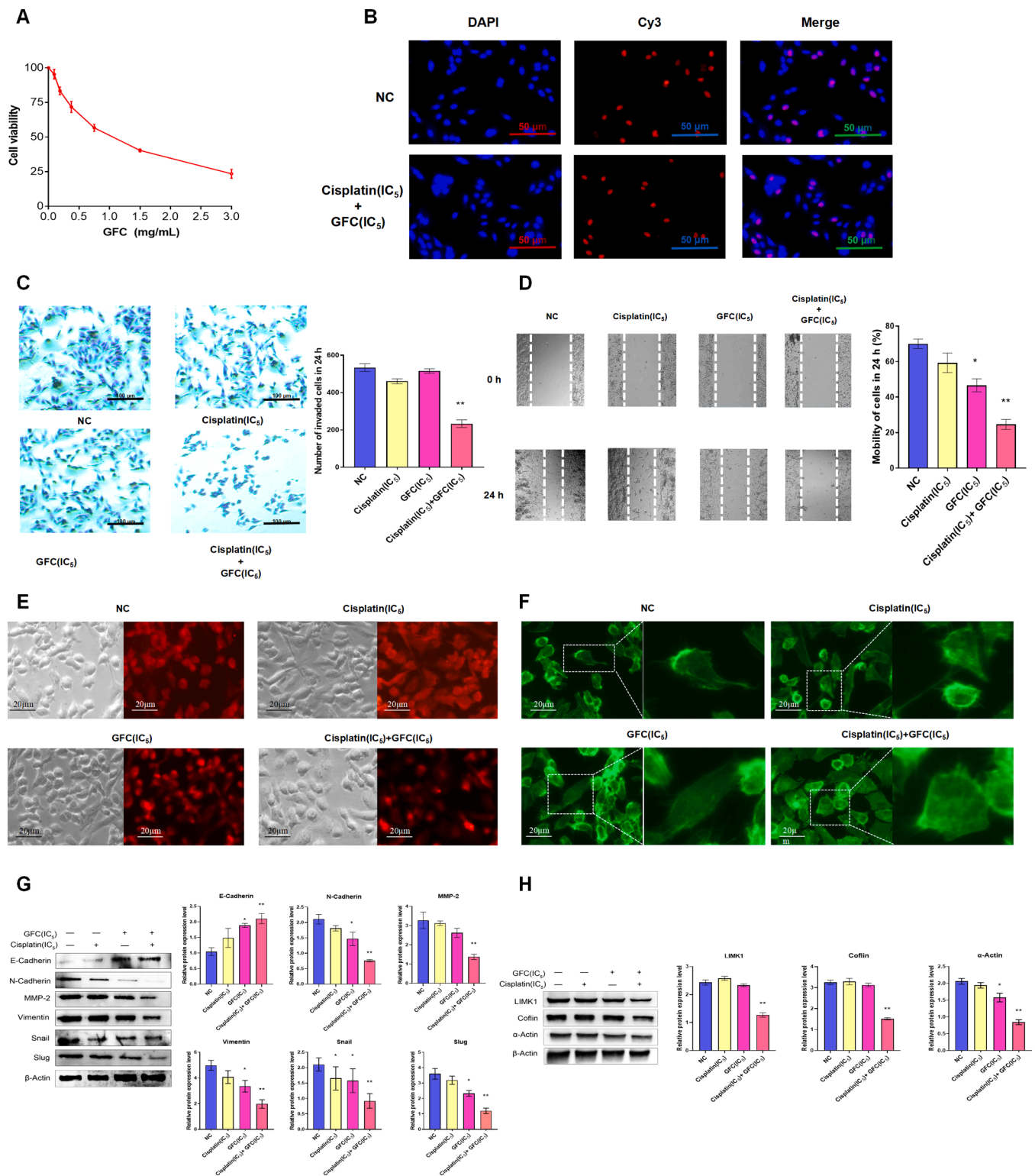
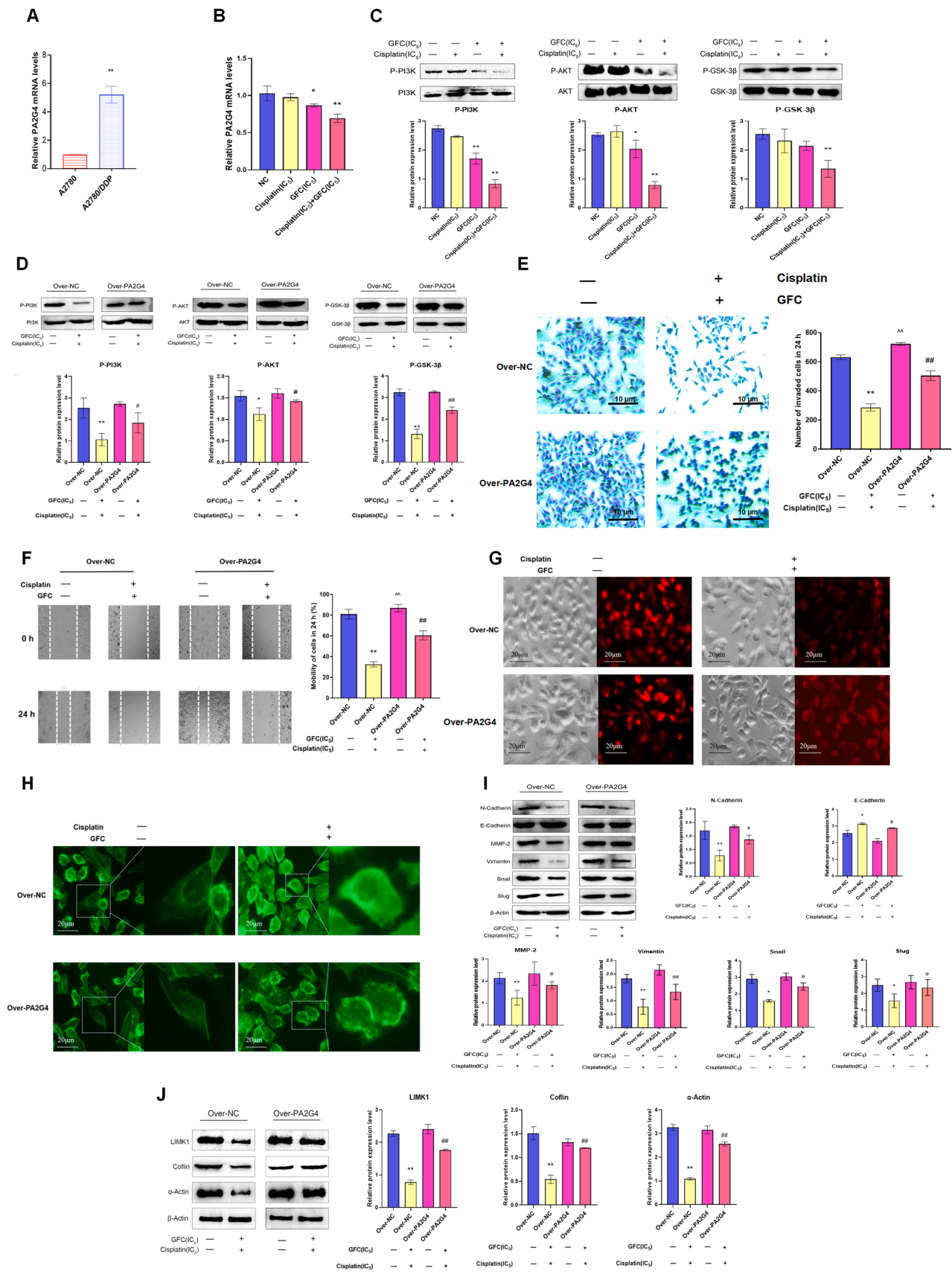


**Fig. 4.** GFC combined with cisplatin can inhibit the invasion and migration of A2780/DDP cells. The effect of GFC on the proliferation of A2780/DDP cells was detected by CCK-8 method (A). EdU assay was used to detect the effect of GFC and cisplatin on the proliferation of A2780/DDP cells (B). Transwell assay to determine the invasion (C). Scratch test to determine the migration (D). Intercellular adhesion was detected by immunofluorescence assay(E). The pseudopodia were detected by fluorescence method(F). Western blot was used to analyze the expression levels of EMT-related proteins(G) and pseudopod-related proteins(H). The experimental results were performed in triplicate, and the results are expressed as mean ± standard deviation. ImageJ software was used to determine the invasion number and the cell migration rate of A2780/DDP cells, and GraphPad Prism 8 was used for statistical analysis of the data. β-actin was the internal reference. ImageJ software statistics protein gray value, and GraphPad Prism 8 was used for statistical analysis of the data.



(caption on next page)

**Fig. 5.** GFC combined with cisplatin can inhibit the PI3K/AKT/GSK-3 $\beta$  signaling pathway and PA2G4 gene in A2780/DDP cells. RT-qPCR was used to detect the expression level of PA2G4 gene in A2780 cells and A2780/DDP cells (A). RT-qPCR detection of the effect of GFC combined with cisplatin on the expression level of PA2G4 gene in A2780/DDP cells (B). Western blot analysis of P-PI3K/PI3K protein expression level, P-AKT/AKT protein expression level and P-GSK-3 $\beta$ /GSK-3 $\beta$  protein expression level(C). The experiment of over-PA2G4 confirmed that GFC combined with cisplatin inhibited the PI3K/AKT/GSK-3 $\beta$  signaling pathway in A2780/DDP cells(D). Transwell assay to determine the invasion (E). Scratch test to determine the migration (F). Inter-cellular adhesion was detected by immunofluorescence assay(G). The pseudopodia were detected by fluorescence method(H). Western blot was used to analyze the expression levels of EMT-related proteins(I) and pseudopod-related proteins(J). The experiment was repeated three times, and the results are expressed as mean  $\pm$  standard deviation.  $\beta$ -actin was the internal reference. ImageJ software statistics protein gray value, and GraphPad Prism 8 was used for statistical analysis of the data. Phosphatidylinositol kinase, PI3K; Serine/threonine kinase, AKT; Serine/threonine kinase, GSK-3 $\beta$ ; phosphorylation, P.

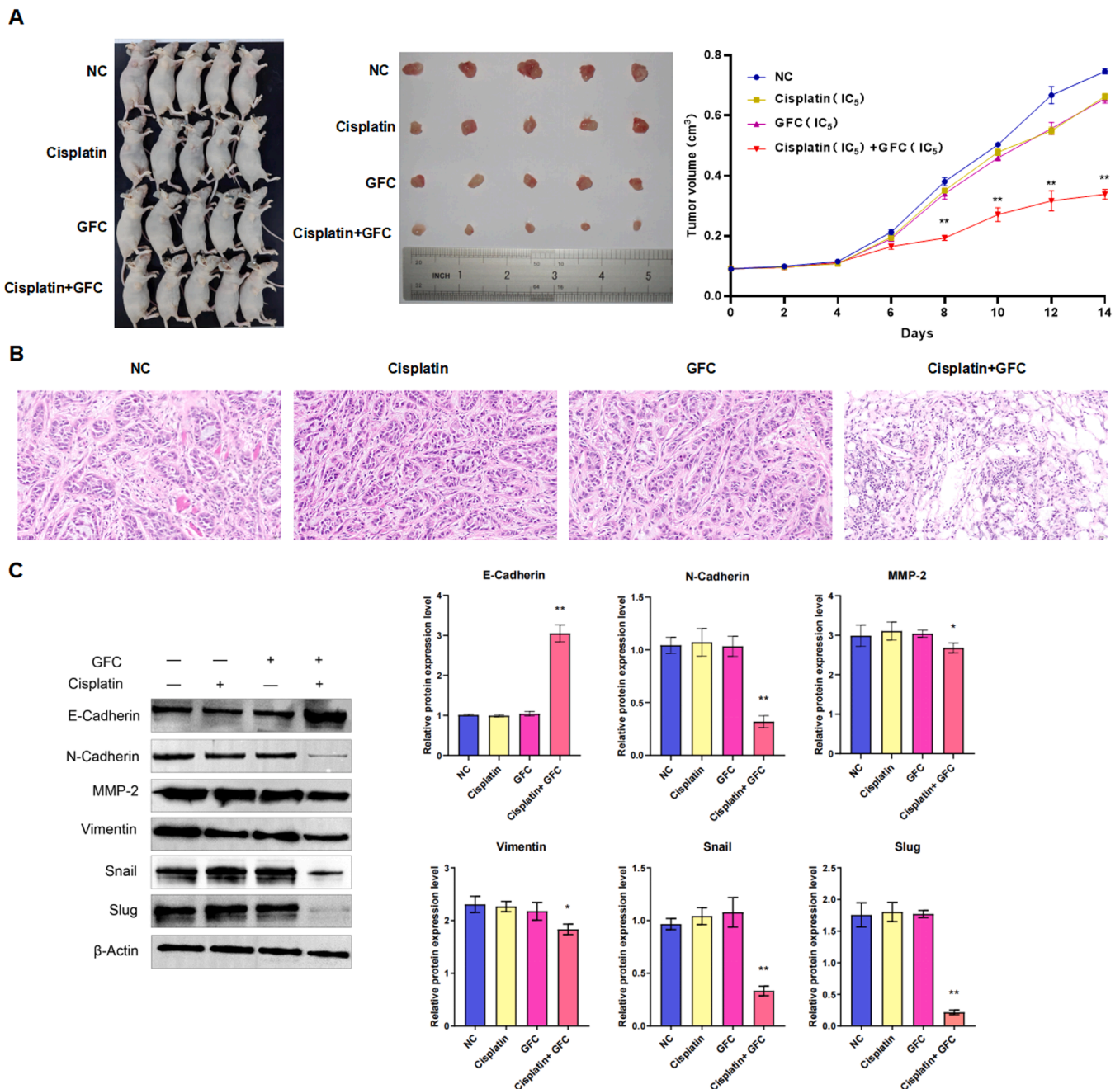


**Fig. 6.** In vivo experiment GFC combined cisplatin antitumor effect. Tumor growth in mice(A). Tumor tissues of mice were stained with HE(B). The protein expression levels of tumor tissues were detected by western blot(C). The experiment was repeated three times, and the results are expressed as mean  $\pm$  standard deviation.  $\beta$ -actin was the internal reference. ImageJ software statistics protein gray value, and GraphPad Prism 8 was used for statistical analysis of the data.

field of medicine in China and other countries. GFC has been used for thousands of years as a traditional Chinese medicine. Modern pharmacological studies have shown that the drug can significantly reduce

blood viscosity, regulate female endocrine diseases, treat gynecological inflammatory diseases, improve immunity, improve cerebral ischemic damage, and inhibit spontaneous hypertension [57]. In addition, recent

studies have shown that GFC can inhibit various tumors [58–61]. It can be used in combination with chemotherapeutic drugs to improve the sensitivity to chemotherapeutic drugs, reduce the occurrence of chemotherapeutic drug resistance, improve the patients' quality of life, and prolong the survival rate [62,63]. In this study, we confirmed that GFC combined with cisplatin was able to reduce the invasion number and the migration rate of A2780/DDP cells by Transwell and scratch experiments. Immunofluorescence analysis showed that the combination of drugs could promote the adhesion of A2780/DDP cells and inhibit the formation of pseudopodia. In addition, we detected the effect of GFC combined with cisplatin on the PI3K/AKT/GSK-3 $\beta$  signaling pathway by western blot. The results showed that the combination of drugs significantly inhibited P-PI3K, P-AKT, and P-GSK-3 $\beta$  protein expression. We also used Western blot to detect the expression of regulatory proteins related to adhesion and pseudopod formation downstream of the PI3K/AKT/GSK-3 $\beta$  signaling pathway after GFC combined with cisplatin treatment. The results showed that the protein expressions of N-cadherin, MMP-2, Vimentin, Snail, Slug, LIMK1, Cofilin and  $\alpha$ -Actin were significantly inhibited by GFC combined with cisplatin, while the protein expression of E-cadherin was significantly increased. The expression of PA2G4 gene in clinical tumor samples was analyzed. Its expression was elevated in many tumor tissues, including cholangiocarcinoma, breast cancer, lung cancer, gastric cancer, and liver cancer. However, the expression level of PA2G4 gene was not significantly different between normal tissues and ovarian tumors, but the expression level of PA2G4 gene in grade 3 ovarian tumors was significantly higher than that in grade 2 ovarian tumors. We compared A2780 cells and A2780/DDP cells by qRT-PCR and found that the expression level of PA2G4 mRNA was significantly higher in A2780/DDP cells. GFC combined with cisplatin was able to significantly inhibit the expression of PA2G4. Compared with the Over-PA2G4 single-action group and the Over-NC+ combination group, after transfection of the Over-PA2G4+ combination, the PI3K/AKT/GSK-3 $\beta$  signaling pathway, adhesion and pseudopodia regulated proteins expression, and the combination of GFC with Cisplatin inhibited the PI3K/AKT/GSK-3 $\beta$  signaling pathway in A2780/DDP cells by targeting the PA2G4 gene, thereby reducing cell invasion and migration.

This study is based on the first-line work of gynecological tumors for many years, which has theoretical and practical significance for solving the problems of gynecological tumors. The frequent drug resistance of ovarian cancer seriously affects the quality of life and survival time of women. Gene targeted therapy, as one of the important means of precision medicine treatment, can reduce the occurrence of tumor drug resistance. In the future, PA2G4 can be used as a biomarker for the prognosis of ovarian cancer. GFC used in this study is widely used in the treatment of gynecological diseases. However, there is no complete and systematic explanation of its pharmacological mechanism reported in the literature, including this study. GFC, as a traditional Chinese medicine compound, has many active ingredients. In the future, public databases and network pharmacology can be used to explore its anti-tumor mechanism. In summary, these results indicate that GFC combined with cisplatin can inhibit the invasion and migration of ovarian cancer cisplatin-resistant A2780/DDP cell line.

## Conclusions

This study showed that high expression of PA2G4 gene and PI3K/AKT/GSK-3 $\beta$  signaling pathway can promote the invasion and migration ability of cisplatin-resistant ovarian cancer cell line A2780/DDP. By targeting PA2G4 gene, GFC combined with cisplatin regulates PI3K/AKT/GSK-3 $\beta$  signaling pathway to inhibit the adhesion between A2780/DDP cells and the formation of pseudopod, thereby inhibiting cell invasion and migration, thus improving the therapeutic effect of cisplatin and providing theoretical basis for the treatment of cisplatin resistant ovarian cancer.

## Animal care were followed in this study

This study was conducted at the School of Life Sciences and Health at Northeastern University in accordance with the Declaration of Helsinki and approved by the local Council of Governance (no. NEU-EC-2023A079S). Their care during research on animals follows ARRIVE guidelines and is conducted in accordance with the National Institutes of Health Guidelines for the Care and Use of Laboratory Animals (NIH Publication No. 8023, as revised in 1978).

## Clinical trial number

Not applicable.

## Abbreviations

GFC	Guizhi Fuling capsule	EMT	Epithelial–mesenchymal transition
DDP	Diamminedichloro platinum	GFW	Guizhi Fuling wan
PA2G4	Recombinant Proliferation Associated Protein 2G4	LncRNA TPT1-AS1	Long non-coding RNA tumor protein Translationally controlled 1 antisense RNA 1
PI3K	Phosphoinositide-3 kinase	miR-671–5p	MicroRNA-671–5p
AKT	Serine/threonine kinase	NRF2	Nuclear factor erythroid 2-related factor 2
GSK-3 $\beta$	Glycogen synthase kinase-3 $\beta$	ULACAN	University of ALabama at Birmingham CANcer
GFD	Guizhi Fuling decoction	EdU	5-Ethynyl-2'-deoxyuridine
RT-qPCR	Real time quantitative	IC	Inhibitory concentration
MMP-2	Matrix metalloproteinase-2	N-cadherin	Neural-cadherin
NF- $\kappa$ B	Nuclear factor kappa-B	E-cadherin	Epithelial-cadherin
PTEN	Phosphatase and tensin homolog		

## CRedit authorship contribution statement

**Lei Dou:** Writing – original draft, Methodology. **Yan Yan:** Writing – review & editing, Software, Investigation. **Enting Lu:** Software, Investigation. **Fangmei Li:** Investigation. **Dongli Tian:** Methodology. **Lei Deng:** Software. **Xue Zhang:** Methodology. **Rongjin Zhang:** Methodology. **Yin Li:** Methodology, Conceptualization. **Yi Zhang:** Funding acquisition, Conceptualization. **Ye Sun:** Writing – review & editing, Writing – original draft, Software, Methodology, Investigation, Conceptualization.

## Declaration of competing interest

The authors declare that there are no conflict of interests, we do not have any possible conflicts of interest

## Data availability

Share the all figures code for the result validation.

## Funding declaration

This work was financially supported by Key Research and Development Project of Liaoning Province (2024JH2/102500019), 2022 Shenyang Science and Technology Plan (22–321–33–08), and Shenyang Bureau of Science and Technology (2023 Special Project to Assist China Medical University in High-quality Development, 23–506–3–01–10). We thank LetPub ([www.letpub.com](http://www.letpub.com)) for its linguistic assistance during

the preparation of this manuscript.

## References

- [1] S M Penny, Ovarian cancer: an overview, *Radiol. Technol.* 91 (6) (2020) 561–575. PMID: 32606233.
- [2] B J Monk, N Colombo, AM Oza, et al., Chemotherapy with or without avelumab followed by avelumab maintenance versus chemotherapy alone in patients with previously untreated epithelial ovarian cancer (JAVELIN Ovarian 100): an open-label, randomised, phase 3 trial, *Lancet Oncol.* 22 (9) (2021) 1275–1289, [https://doi.org/10.1016/S1470-2045\(21\)00342-9](https://doi.org/10.1016/S1470-2045(21)00342-9).
- [3] M S Schuurman, RFPM Kruitwagen, JEA Portielje, et al., Treatment and outcome of elderly patients with advanced stage ovarian cancer: A nationwide analysis, *Gynecol. Oncol.* 149 (2) (2018) 270–274, <https://doi.org/10.1016/j.ygyno.2018.02.017>.
- [4] J Y Kim, C H Cho, H S Song, Targeted therapy of ovarian cancer including immune check point inhibitor, *Korean J. Intern Med.* 32 (5) (2017) 798–804, <https://doi.org/10.3904/kjim.2017.008>.
- [5] E Hamilton, D M O'Malley, R O'Carbhaill, et al., Tamrintamab pamozirine (SC-003) in patients with platinum-resistant/refractory ovarian cancer: Findings of a phase 1 study, *Gynecol. Oncol.* 158 (3) (2020) 640–645, <https://doi.org/10.1016/j.ygyno.2020.05.038>.
- [6] M. Moghbeli, MicroRNAs as the critical regulators of Cisplatin resistance in ovarian cancer cells, *J. Ovarian Res.* 14 (1) (2021) 127, <https://doi.org/10.1186/s13048-021-00882-1>.
- [7] M Kleih, K Böppe, M Dong, et al., Direct impact of cisplatin on mitochondria induces ROS production that dictates cell fate of ovarian cancer cells, *Cell Death Dis.* 10 (11) (2019) 851, <https://doi.org/10.1038/s41419-019-2081-4>.
- [8] X Zhang, L Liu, M Tang, et al., The effects of umbilical cord-derived macrophage exosomes loaded with cisplatin on the growth and drug resistance of ovarian cancer cells, *Drug. Dev. Ind. Pharm.* 46 (7) (2020) 1150–1162, <https://doi.org/10.1080/03639045.2020.1776320>.
- [9] G Babaei, S G Aziz, N Z Z Jaghi, EMT, cancer stem cells and autophagy; The three main axes of metastasis, *Biomed. Pharmacother.* 133 (2021) 110909, <https://doi.org/10.1016/j.biopha.2020.110909>.
- [10] M Suarez-Carmona, J Lesage, D Cataldo, et al., EMT and inflammation: inseparable actors of cancer progression, *Mol. Oncol.* 11 (7) (2017) 805–823, <https://doi.org/10.1002/1878-0261.12095>.
- [11] S Roy, R R Sunkara, M Y Parmar, et al., EMT imparts cancer stemness and plasticity: new perspectives and therapeutic potential, *Front Biosci.* 26 (2) (2021) 238–265, <https://doi.org/10.2741/4893>.
- [12] I Pastushenko, C Blanpain, EMT Transition States during Tumor Progression and Metastasis, *Trends Cell Biol.* 29 (3) (2019) 212–226, <https://doi.org/10.1016/j.tcb.2018.12.001>.
- [13] M. Saitoh, Involvement of partial EMT in cancer progression, *J. Biochem.* 164 (4) (2018) 257–264, <https://doi.org/10.1093/jb/mvy047>.
- [14] G Pan, Y Liu, L Shang, et al., EMT-associated microRNAs and their roles in cancer stemness and drug resistance, *Cancer Commun.* 41 (3) (2021) 199–217, <https://doi.org/10.1002/cac2.12138>.
- [15] T Shibue, R A Weinberg, EMT, CSCs, and drug resistance: the mechanistic link and clinical implications, *Nat Rev. Clin. Oncol.* 14 (10) (2017) 611–629, <https://doi.org/10.1038/nrclinonc.2017.44>.
- [16] M E Fiori, S Di Franco, L Villanova, et al., Cancer-associated fibroblasts as abettors of tumor progression at the crossroads of EMT and therapy resistance, *Mol. Cancer* 18 (1) (2019) 70, <https://doi.org/10.1186/s12943-019-0994-2>.
- [17] P Zhou, B Li, F Liu, et al., The epithelial to mesenchymal transition (EMT) and cancer stem cells: implication for treatment resistance in pancreatic cancer, *Mol. Cancer* 16 (1) (2017) 52, <https://doi.org/10.1186/s12943-017-0624-9>.
- [18] A Dongre, R A Weinberg, New insights into the mechanisms of epithelial-mesenchymal transition and implications for cancer, *Nat. Rev. Mol. Cell Biol.* 20 (2) (2019) 69–84, <https://doi.org/10.1038/s41580-018-0080-4>.
- [19] M Najafi, K Mortezaee, J. Majidpoor, Cancer stem cell (CSC) resistance drivers, *Life Sci.* 234 (2019) 116781, <https://doi.org/10.1016/j.lfs.2019.116781>.
- [20] T K Sahin, A Rizzo, S Aksoy, et al., Prognostic significance of the royal Marsden hospital (RMH) score in patients with cancer: a systematic review and meta-analysis, *Cancers* 16 (10) (2024) 1835, <https://doi.org/10.3390/cancers16101835>.
- [21] D C Guven, E Erul, Y Kayguzuz, et al., Immune checkpoint inhibitor-related hearing loss: a systematic review and analysis of individual patient data, *Supp. Care Cancer* 31 (12) (2023) 624, <https://doi.org/10.1007/s00520-023-08083-w>.
- [22] A Rizzo, M Santoni, V Mollica, et al., Peripheral neuropathy and headache in cancer patients treated with immunotherapy and immuno-oncology combinations: the MOUSEION-02 study, *Expert Opin. Drug Metab. Toxicol.* 17 (12) (2021) 1455–1466, <https://doi.org/10.1080/17425255.2021.2029405>.
- [23] A. Rizzo, Immune checkpoint inhibitors and mismatch repair status in advanced endometrial cancer: elective affinities, *J. Clin. Med.* 11 (13) (2022) 3912, <https://doi.org/10.3390/jcm11133912>.
- [24] A Rizzo, V Mollica, V Tateo, et al., Hypertransaminasemia in cancer patients receiving immunotherapy and immune-based combinations: the MOUSEION-05 study, *Cancer Immunol. Immunother.* 72 (6) (2023) 1381–1394, <https://doi.org/10.1007/s00262-023-03366-x>.
- [25] N N Chen, M Han, H Yang, et al., Chinese herbal medicine Guizhi Fuling Formula for treatment of uterine fibroids: a systematic review of randomised clinical trials, *BMC Compl. Altern Med.* 14 (2014) 2, <https://doi.org/10.1186/1472-6882-14-2>.
- [26] W Zheng, M Li, Y Wang, et al., Guizhi fuling capsule exhibits antidysmenorrhea activity by inhibition of cyclooxygenase activity, *Evid. Based Compl. Alternat Med.* 2020 (2020) 8607931, <https://doi.org/10.1155/2020/8607931>.
- [27] B. Zhang, Guizhi Fuling pills inhibit the proliferation, migration and invasion of human cutaneous malignant melanoma cells by regulating the molecular axis of LncRNA TPT1-AS1/miR-671-5p, *Cell Mol. Biol. (Noisy-le-grand)* 66 (5) (2020) 148–154. PMID: 33040829.
- [28] M Zhang, T Zhang, C Song, et al., Guizhi Fuling Capsule ameliorates endometrial hyperplasia through promoting p62-Keap1-NRF2-mediated ferroptosis, *J. Ethnopharmacol.* 274 (2021) 114064, <https://doi.org/10.1016/j.jep.2021.114064>.
- [29] A M Tsimberidou, E Fountzilias, M Nikanjam, et al., Review of precision cancer medicine: Evolution of the treatment paradigm, *Cancer Treat Rev.* 86 (2020) 102019, <https://doi.org/10.1016/j.ctrv.2020.102019>.
- [30] M A Zaimy, N Saffarzadeh, A Mohammadi, et al., New methods in the diagnosis of cancer and gene therapy of cancer based on nanoparticles, *Cancer Gene Ther.* 24 (6) (2017) 233–243, <https://doi.org/10.1038/cgt.2017.16>.
- [31] C de Castro Sant' Anna, AGF Junior, P Soares, et al., Molecular biology as a tool for the treatment of cancer, *Clin. Exp. Med.* 18 (4) (2018) 457–464, <https://doi.org/10.1007/s10238-018-0518-1>.
- [32] E Pérez-Herrero, A. Fernández-Medarde, Advanced targeted therapies in cancer: Drug nanocarriers, the future of chemotherapy, *Eur. J. Pharm. Biopharm.* 93 (2015) 52–79, <https://doi.org/10.1016/j.ejpb.2015.03.018>.
- [33] N R Datta, B Pestalozzi, P A Clavien, et al., HEATPAC - a phase II randomized study of concurrent thermochemoradiotherapy versus chemoradiotherapy alone in locally advanced pancreatic cancer, *Radiat. Oncol.* 12 (1) (2017) 183, <https://doi.org/10.1186/s13014-017-0923-8>.
- [34] S Dasari, P B T'chounwou, Cisplatin in cancer therapy: molecular mechanisms of action, *Eur. J. Pharmacol.* 740 (2014) 364–378, <https://doi.org/10.1016/j.ejphar.2014.07.025>.
- [35] L Qi, Q Luo, Y Zhang, et al., Advances in toxicological research of the anticancer drug cisplatin, *Chem. Res. Toxicol.* 32 (8) (2019) 1469–1486, <https://doi.org/10.1021/acs.chemrestox.9b00204>.
- [36] H Zhu, H Luo, W Zhang, et al., Molecular mechanisms of cisplatin resistance in cervical cancer, *Drug Des Devel. Ther.* 10 (2016) 1885–1895, <https://doi.org/10.2147/DDDT.S106412>.
- [37] L Galluzzi, L Senovilla, I Vitale, et al., Molecular mechanisms of cisplatin resistance, *Oncogene* 31 (15) (2012) 1869–1883, <https://doi.org/10.1038/onc.2011.384>.
- [38] V. Mittal, Epithelial Mesenchymal Transition in Tumor Metastasis, *Annu. Rev. Pathol.* 13 (2018) 395–412, <https://doi.org/10.1146/annurev-pathol-020117-043854>.
- [39] S Lamouille, J Xu, R Derynck, Molecular mechanisms of epithelial-mesenchymal transition, *Nat. Rev. Mol. Cell Biol.* 15 (3) (2014) 178–196, <https://doi.org/10.1038/nrm3758>.
- [40] Y Zhang, R A Weinberg, Epithelial-to-mesenchymal transition in cancer: complexity and opportunities, *Front Med.* 12 (4) (2018) 361–373, <https://doi.org/10.1007/s11684-018-0656-6>.
- [41] S Usman, N H Waseem, T K N Nguyen, et al., Vimentin Is at the Heart of Epithelial Mesenchymal Transition (EMT) Mediated Metastasis, *Cancers (Basel)* 13 (19) (2021) 4985, <https://doi.org/10.3390/cancers13194985>.
- [42] J Cai, Y Cui, J Yang, et al., Epithelial-mesenchymal transition: When tumor cells meet myeloid-derived suppressor cells, *Biochim. Biophys. Acta Rev. Cancer* 1876 (1) (2021) 188564, <https://doi.org/10.1016/j.bbcan.2021.188564>.
- [43] N A Gloushankova, I Y Zhitnyak, S N Rubtsova, Role of Epithelial-Mesenchymal transition in tumor progression, *Biochemistry* 83 (12) (2018) 1469–1476, <https://doi.org/10.1134/S0006297918120052>.
- [44] S Brabletz, H Schuhwerk, T Brabletz, et al., Dynamic EMT: a multi-tool for tumor progression, *EMBO J.* 40 (18) (2021) e108647, <https://doi.org/10.15252/emj.2021108647>.
- [45] D Yao, C Dai, S. Peng, Mechanism of the mesenchymal-epithelial transition and its relationship with metastatic tumor formation, *Mol. Cancer Res.* 9 (12) (2011) 1608–1620, <https://doi.org/10.1158/1541-7786.MCR-10-0568>.
- [46] J Yang, J Nie, X Ma, et al., Targeting PI3K in cancer: mechanisms and advances in clinical trials, *Mol. Cancer* 18 (1) (2019) 26, <https://doi.org/10.1186/s12943-019-0954-x>.
- [47] S Revathidevi, A K Munirajan, Akt in cancer: Mediator and more, *Semin Cancer Biol.* 59 (2019) 80–91, <https://doi.org/10.1016/j.semcancer.2019.06.002.5>.
- [48] M Martini, M C De Santis, L Braccini, et al., PI3K/AKT signaling pathway and cancer: an updated review, *Ann. Med.* 46 (6) (2014) 372–383, <https://doi.org/10.3109/07853890.2014.912836>.
- [49] A G Abraham, E O'Neill, PI3K/Akt-mediated regulation of p53 in cancer, *Biochem. Soc. Trans.* 42 (4) (2014) 798–803, <https://doi.org/10.1042/BST20140070>.
- [50] S A Danielsen, P W Eide, A Nesbakken, et al., Portrait of the PI3K/AKT pathway in colorectal cancer, *Biochim. Biophys. Acta* 1855 (1) (2015) 104–121, <https://doi.org/10.1016/j.bbcan.2014.09.008>.
- [51] M K Ediriweera, K H Tennekoon, S R Samarakoon, Role of the PI3K/AKT/mTOR signaling pathway in ovarian cancer: Biological and therapeutic significance, *Semin Cancer Biol* 59 (2019) 147–160, <https://doi.org/10.1016/j.semcancer.2019.05.012>.
- [52] M Yu, B Qi, W Xiaoxiang, et al., Baicalein increases cisplatin sensitivity of A549 lung adenocarcinoma cells via PI3K/Akt/NF-κB pathway, *Biomed. Pharmacother.* 90 (2017) 677–685, <https://doi.org/10.1016/j.biopha.2017.04.001>.
- [53] Y Y Shi, X T Meng, Y N Xu, et al., Role of FOXO protein's abnormal activation through PI3K/AKT pathway in platinum resistance of ovarian cancer, *J. Obstet Gynaecol. Res.* 47 (6) (2021) 1946–1957, <https://doi.org/10.1111/jog.14753>.

- [54] J Lin, T Song, C Li, et al., GSK-3 $\beta$  in DNA repair, apoptosis, and resistance of chemotherapy, radiotherapy of cancer, *Biochim. Biophys. Acta Mol. Cell Res.* 1867 (5) (2020) 118659, <https://doi.org/10.1016/j.bbamcr.2020.118659>.
- [55] L Liu, T Meng, X Zheng, et al., Transgelin 2 promotes paclitaxel resistance, migration, and invasion of breast cancer by directly interacting with PTEN and activating PI3K/Akt/GSK-3 $\beta$  pathway, *Mol. Cancer Ther.* 18 (12) (2019) 2457–2468, <https://doi.org/10.1158/1535-7163.MCT-19-0261>.
- [56] A Wei, B Fan, Y Zhao, et al., ST6Gal-I overexpression facilitates prostate cancer progression via the PI3K/Akt/GSK-3 $\beta$ / $\beta$ -catenin signaling pathway, *Oncotarget* 7 (40) (2016) 65374–65388, <https://doi.org/10.18632/oncotarget.11699>.
- [57] F Tao, S Ruan, W Liu, et al., Fuling Granule, a Traditional Chinese Medicine Compound, Suppresses Cell Proliferation and TGF $\beta$ -Induced EMT in Ovarian Cancer, *PLoS ONE* 11 (12) (2016) e0168892, <https://doi.org/10.1371/journal.pone.0168892>.
- [58] B. Zhang, Guizhi Fuling pills inhibit the proliferation, migration and invasion of human cutaneous malignant melanoma cells by regulating the molecular axis of lncRNA TPT1-AS1 /miR-671-5p, *Cell Mol. Biol. (Noisy-le-grand)* 66 (5) (2020) 148–154.
- [59] Y Dai, W Qiang, X Yu, et al., Guizhi Fuling Decoction inhibiting the PI3K and MAPK pathways in breast cancer cells revealed by HTS2 technology and systems pharmacology, *Comput. Struct. Biotechnol. J.* 18 (2020) 1121–1136, <https://doi.org/10.1016/j.csbj.2020.05.004>.
- [60] Z Yao, Z. Shulan, Inhibition effect of Guizhi-Fuling-decoction on the invasion of human cervical cancer, *J. Ethnopharmacol.* 120 (1) (2008) 25–35, <https://doi.org/10.1016/j.jep.2008.07.044>.
- [61] L Han, X Cao, Z Chen, et al., Overcoming cisplatin resistance by targeting the MTDH-PTEN interaction in ovarian cancer with sera derived from rats exposed to Guizhi Fuling wan extract, *BMC Compl. Med. Ther.* 20 (1) (2020) 57, <https://doi.org/10.1186/s12906-020-2825-9>.
- [62] Y Zhu, Y Li, M Liu, et al., Guizhi Fuling Wan, Chinese Herbal Medicine, Ameliorates Insulin Sensitivity in PCOS Model Rats With Insulin Resistance via Remodeling Intestinal Homeostasis, *Front Endocrinol. (Lausanne)* 11 (2020) 575, <https://doi.org/10.3389/fendo.2020.00575>.
- [63] L Han, X Cao, Z Chen, et al., Overcoming cisplatin resistance by targeting the MTDH-PTEN interaction in ovarian cancer with sera derived from rats exposed to Guizhi Fuling wan extract, *BMC Compl. Med. Ther.* 20 (1) (2020) 57, <https://doi.org/10.1186/s12906-020-2825-9>.